Analysis of Mutual Inductance for Inductive Coupled Dynamically Charged Varying Speed Electric Vehicle

Hassan Khalid
Power Electronics and Renewable Energy Research Laboratory (PEARL), Department of Electrical Engineering, University of Malaya, Kuala Lumpur 50603, Malaysia
School of Software and Electrical Engineering, Swinburne University of Technology, Melbourne, VIC 3122, Australia
khalid.hassan18@yahoo.com

Saad Mekhilef
School of Software and Electrical Engineering, Swinburne University of Technology, Melbourne, VIC 3122, Australia.
Power Electronics and Renewable Energy Research Laboratory (PEARL), Department of Electrical Engineering, University of Malaya, Kuala Lumpur 50603, Malaysia. smekhilef@swin.edu.au

Mehdi Seyedmahmoudian
School of Software and Electrical Engineering, Swinburne University of Technology, Melbourne, VIC 3122, Australia
mseyedmahmoudian@swin.edu.au

Alex Stojcevski
School of Software and Electrical Engineering, Swinburne University of Technology, Melbourne, VIC 3122, Australia
astojcevski@swin.edu.au

Marizan Binti Mubin
Power Electronics and Renewable Energy Research Laboratory (PEARL), Department of Electrical Engineering, University of Malaya, Kuala Lumpur 50603, Malaysia
marizan@um.edu.my

Peyman Darvish
Power Electronics and Renewable Energy Research Laboratory (PEARL), Department of Electrical Engineering, University of Malaya, Kuala Lumpur 50603, Malaysia.
peymandarvish@um.edu.my

Amran Hossain
Power Electronics and Renewable Energy Research Laboratory (PEARL), Department of Electrical Engineering, University of Malaya, Kuala Lumpur 50603, Malaysia.
amranhossain@um.edu.my

***Abstract*—The inductive power transfer for dynamically charged electric vehicles has solved major of the issues encountered during static and wired-based electric vehicle charging. However, dynamic charging is still facing challenges during high-speed receiver displacement over the transmitter. The high-speed receiver requires a high response receiver design. This requires certain modifications in the receiver coil. Therefore, this paper proposes a mathematical model to visualize factors affecting receiver performance during velocity variation. In this regard, various simulation tools including MATLAB, ANSYS Maxwell and LTSpice have helped to identify controlling parameters. Based on simulation results the inductance variation is recommended to optimize power receiving capacity.**

***Index Terms*— Dynamic charging, Electric vehicle, Velocity Wireless power transfer.**

I. INTRODUCTION

The recent advancements in wireless power technology have now started to replace big connectors with small and smart wireless power transfer (WPT) charging pads. Moreover, cellular mobiles, tablets and other smart applications have now become more compact so that batteries are charged by placing them on the surface of the table. The wireless power transfer neither requires any medium to propagate nor is affected by environmental conditions. The WPT is done by using any one of the methods like capacitive power transfer (CPT), inductive power transfer (IPT), optical power transfer (OPT), microwave power transfer (MPT), or resonant inductive power transfer (RIPT). Each of these techniques differs in terms of frequency, power transfer capacity and air gap support between primary and secondary coils [1]. Due to many of the benefits offered by capacitive and resonant inductive power transfer. Any of the methods is preferable. In CPT, two metallic plates are used to form a capacitor with air as a dielectric medium between plates and power is transferred using the electric field. At first, it has the inherent ability to achieve a unity power factor and is least sensitive to plate misalignment. However, it has certain limitations. To enhance capacitance, a high-frequency range (kHz—MHz) is required. Secondly, the air-gap support is less than RIPT. Alternatively, RIPT has a high capacity to transfer power, even does not require a high resonant frequency range, and can transfer at a distance of less than a meter.

The current plugin electric vehicles (EV) along with high gain DC converters to charge EV batteries [2] are available in the market but these are limited due to battery backup and its cost. Dynamic charging on other hand overcomes these issues.

Unlike static charging, dynamic charging has certain challenges. First, it requires a highly efficient coil to maximize power transfer. The ideal coupling factor (k) must be unity, the mutual inductance between coils must be high and finally, yet importantly, its characteristics must not be affected by the load variation. However, the coupling and mutual inductance of the coil depend on the geometry of the coil. To evaluate these parameters numerical analysis is applied using ANSYS Maxwell tools. Secondly, coil utilization depends on the type of compensation. There are four basic topologies comprising capacitors and inductors either in series (S) or in parallel (P) [3]. However, other topologies include SPS, LCC, and LCL [4], [5]. Among these topologies, the conventional SS and SP are considered good methods to transfer high power and at higher efficiencies. While PP and PS are used for moderate power levels and have lower efficiencies [6]. However, SS and SP topologies are not recommended in dynamic applications. The major concern is a very high circulating current in the primary side upon misalignment. In dynamic charging, the receiver pad slides over the transmitter and as the misalignment occurs, the inverter current will shoot high which is not desirable. To

978-1-6654-6738-4/22/$31.00 ©2022 IEEE

overcome this issue SPS was preferred. Later on, LCL and LCC-type compensation were mostly used. Both of these topologies almost offer the same benefits. However, LCC leads LCL by reducing additional air-core inductors. In LCC, type compensation of the resonant frequency (f_r) is independent of k and load. Unlike SS-type compensation, LCC compensation offers great support against misalignment and improves air-gap support. However, turn off current $(I_{turn-off})$ is higher and needs to be minimum at the time of zero voltage switching (ZVS). In addition, these compensation networks are widely used during static charging. But most of the existing literature in dynamic charging just concerns variation in mutual inductance concerning multiple transmitters and improving the power transfer pulsation [7], [8], [17], [9]–[16]. However, theoretical analysis of the receiver concerning its relative velocity over the transmitter needs attention.

In this paper, a theoretical analysis based on mathematical formulations are presented to relate receiver-sliding velocity (v_{slide}) under the EV system with that of M; afterwards these results are applied to symmetric double-sided LCC compensation to visualize the behaviour of EV charging. In order to measure the impact of velocity model, LTSpice and ANSYS simulation tools are used for further analysis.

The paper is organized as follows: Section II presents the mathematical model of v_{slide}. Section III presents the system analysis using simulation tools. While section IV concludes the whole discussion.

II. Mathematical Model of the Proposed Scheme

In this section, we will consider the conventional circular coil as an example, which is renowned for maintaining a good range of coupling coefficients. The coil can be either a single coil or multiple coils. These can generate flux in either unidirectional, named unipolar coil. While the coil that generates flux in both directions is a bi-directional coil. All types of coils are developed and distinguished in terms of flux height and direction of generation as summarized in Table I [18]–[23]. Among these coils, DDQ and bipolar type configuration has the highest tolerance and offers twice magnetic field strength as compared to their size. However, the zig-zag coil eliminates the possibility of a null region but as compared to other coil shapes offers minimum flux support.

Table I: Coils designs and characteristics

Coil design	Null region (%)	Flux height, coil size (%)	Flux direction	Coil
Circular	40	25	Unidirectional	Single
Flux pipe	In all directions	50	Bidirectional	Multiple
DD	34	50	Bidirectional	Single
DDQ	95	200	Bidirectional	Multiple
Bipolar	95	200	Bidirectional	Single
Tripolar	Non symmetric	-	Unidirectional	Multiple
Zigzag	No Null	4	Unidirectional	Multiple

According to Faraday's law, the amount of magnetic flux density (B) enclosed by a closed surface having area (A) resulted in magnetic flux (ϕ_B) generation given by (1). Whereas the magnetic flux will be maximum if two coils are perfectly aligned and perpendicular to each other. Hence, (2) gives the total magnetic flux in a uniform surface.

$$\boldsymbol{\phi}_B = \int_0^{A_S} \boldsymbol{B}.dA \tag{1}$$

$$\phi_B = BA \tag{2}$$

From (2), we can define Faraday's law more quantitatively. The magnitude of induced emf (ε) is equal to the rate of change of flux in one loop and for N number of loops in a circular coil in opposite direction as by (3). While the voltage induced in an inductor is given by (4). Therefore, the inductance of any coil can be easily evaluated using (2), (3) and (4) as in (5). The magnetic flux thus generated through any surface also has its strength defined in terms of its intensity called magnetic field intensity (H) and is directly proportional to B *as* in (6). Here, μ is the magnetic permability.

$$\varepsilon = -N\left(\frac{d\phi_B}{dt}\right) \tag{3}$$

$$\varepsilon = -L\left(\frac{di_L}{dt}\right) \tag{4}$$

$$L = \frac{NBA}{i} \tag{5}$$

$$\boldsymbol{B_S} = \mu \boldsymbol{H_S} \tag{6}$$

According to Ampere's law, the line integral of magnetic field intensity in a closed-loop path is cumulative of current flowing in the path. While we can apply this concept over a circular coil with N turns to obtain magnetomotive force *(F)* to relate both current and magnetic field strength as in (7).

$$H_S l = Ni = F \tag{7}$$

Rearranging and writing (7) for a small change of current per unit length as (8). In dynamic, the receiver pad coil slides over other coils with a certain velocity, which also affects the magnetic field and induced emf. Therefore, from (1) to (8), H can be easily mentioned in terms of velocity *(v)* as in (9). It is assumed that from (7) to (9) only magnitude is concerned but not direction.

$$H_S = N\left(\frac{di}{dl}\right) \tag{8}$$

$$H_S(v) = N\left(\frac{di}{dt}\right) \times \frac{dt}{dl} = N\left(\frac{di}{dt}\right) \times \frac{1}{v} = \mathrm{N}\left(\frac{\varepsilon}{L}\right)\frac{1}{v} \tag{9}$$

Considering the receiver coil. In (9), it is clear that as the velocity of EV increases, the magnetic field between transmitter and receiver coil will become weak, due to which the resulting induced voltage will become weak. Hence, the induced current and magnetic flux from (3) and (4) will become weak as well. Therefore, the receiver will not be able to produce enough power to charge the battery.

The velocity of the moving coil can also be realized in terms of magnetically coupled coils. The mutual inductance

(M) and self-inductances of the transmitter (L_T) and receiver (L_R) coils are related by (10). Here, $k \in [0,1]$, suggests that the mutual inductance between transmitter and receiver coils must be as high as coupling becomes unity. Also, L_T, L_R for any coil is obtained from (5). Since the self-inductance of the coils remain constant, the mutual inductance varies with the position of the receiver coil.

$$M(k) = k\sqrt{L_T L_R}, 0 \le k < 1 \tag{10}$$

If the inductance model of the receiver is realized in terms of its received magnetic field intensity(H_R), then the required effective mutual inductance $\left(M_{eff}\right)$ between the coils at the required EV velocity can be easily attained as in (11). Here transmitter side self-inductance is assumed to remain constant.

$$M_{eff}(v) = k\sqrt{\frac{L_T N \mu A}{i} H_R(v)} \tag{11}$$

The next section presents the simulation-based analysis for the proposed model. For the LCC-based compensation, the input to output power flow between coils is given by (12) [9].

$$P = V_{AC_{in}} V_{AC_{out}} k \left(\frac{\sqrt{L_T L_R}}{\omega_o L_{f1} L_{f2}}\right) \tag{12}$$

III. Simulation Analysis and Discussion

The required parameters for the system chosen are mentioned in Table II. While the process flow for design is presented in Fig. 1. The system analysis has been performed with the help of different modelling software, i.e., using MATLAB Math Works. LTSpice is used to analyse system transient analysis. However, ANSYS is adopted to analyse small-scale circular coils using finite element analysis (FEA).

Based on the parameters, the mathematical model thus developed in the previous section is analyzed using graphical analysis tools. In Fig. 2, the required magnetic field intensity (H) and mutual inductance (M) are analyzed as a function of varying EV speed. The area of the transmitter and receiver pad is $625cm^2$. It is connected to the LCC type double-sided compensation as shown in Fig. 3. It is assumed that the receiver will pass by the transmitter pad in $38ms$ at a velocity of $10\,m/s$. Since the separation between the pads is approximately $8.5\,cm$. Therefore, for such velocity, the magnetic field intensity strength received by the receiver must be approximately $315\,A-N/m$. In addition, the mutual inductance between pads during this short time must be around $35\mu H$. As the velocity is further increased, the ability of the receiver to maintain such mutual inductance and electric field intensity will drop significantly.

The parameter evaluation for a double-sided LCC compensation system is based on the resonance frequency principle. At resonance the impedance of $L_{f1,2}$ and $C_{f1,2}$ becomes infinite and the side behaves as the open circuit and is given by (13) and (14). For a double-sided LCC network, the additional inductor size must be at least six times lower than the transmitter coil. Otherwise, both will participate in transmitting power, which is an ultimate loss.

$$C_{f1} = \frac{1}{\omega^2 L_{f1}} \tag{13}$$

$$C_{f2} = \frac{1}{\omega^2 L_{f2}} \tag{14}$$

Similarly, the capacitor (C_1) and (C_2) connected in series to the main coils are evaluated using (15) and (16).

$$C_1 = \frac{1}{\omega^2 (L_1 - L_{f1})} \tag{15}$$

$$C_2 = \frac{1}{\omega^2 (L_2 - L_{f2})} \tag{16}$$

However, the transmitter and receiver current are obtained through KVL as in (17) and (18).

$$I_{transmitter} = \frac{V_{AC_{in}}}{j\omega_o L_{f1}} \tag{17}$$

$$I_{receiver} = -\frac{V_{AC_{out}}}{j\omega_o L_{f2}} \tag{18}$$

As the velocity is further increased, the ability of the receiver to maintain such mutual inductance and electric field intensity will drop significantly.

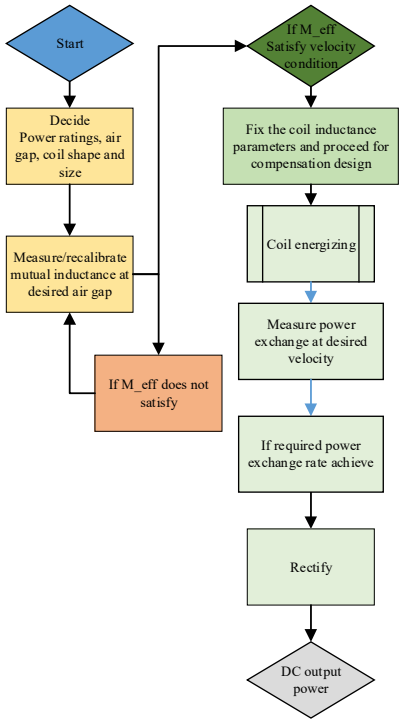

Figure 1: Process flow diagram for designing dynamic wireless power transfer system

TABLE II: PARAMETER SELECTION FOR THE DYNAMIC CHARGING SYSTEM

Parameter	Value	Parameter	Value
Transmitter inductance	$175\mu H$	Receiver inductance	$175\mu H$
L_{f1}	$33\mu H$	L_{f2}	$33\mu H$
C_{f1}	$76.8nC$	C_{f2}	$76.8nC$
C_1	$17.8nC$	C_2	$17.208nC$
Load resistance	45Ω	Diodes (60 V, 15 A)	RF2001NS2D
k	$0.1 - 0.5$	Air gap	8.5 cm
(v_{slide})	$10\ m/s$	Max. coil current	$4A$

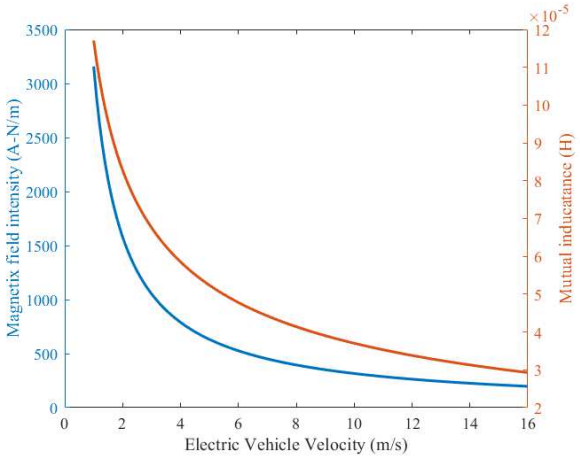

Figure 2: Variation in mutual inductance and magnetic field strength as a function of receiver velocity

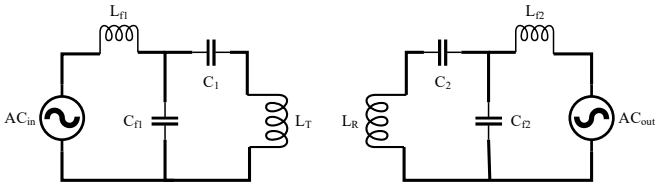

Figure 3: Double sided LCC compensation

The speed not only affects mutual inductance but the ability to receiver power by the receiver is also affected. Writing (12) in terms of mutual inductance to get (19). From (19), the output power received is directly proportional to the effective mutual inductance. Since the air gap was held constant and was assumed that there was only horizontal misalignment, the power significantly drops with the increased velocity. Hence the EV receiver pad traveling at a velocity of $10m/s$, will only be able to receive approximately 135 W. However, for the reduced speed, the receiver can receive a maximum of up to 450 W as in Fig. 4.

$$P = V_{AC_{in}} V_{AC_{out}} \left(\frac{M_{eff}(v)}{\omega_o L_{f1} L_{f2}} \right) \tag{19}$$

Based on the speed analysis, various options can be adopted to optimize speed and received power. 1) The length of the receiver pad can be reduced using (8) to strengthen the magnetic field strength for receiving pad. In this way, the receiver response factor can be easily enhanced. 2) The area of the receiver can be extended to increase its inductance. This will increase the M and hence receiver's power can be enhanced. But increasing L_R will also cause a reduction in magnetic field strength as by (9). Lastly, increasing the number of turns in the receiver can also enhance the receiver response at a higher velocity.

The complete transient analysis at the steady-state of the proposed scheme based on parameters stated in Table II has been simulated using LTSpice. The parameter selection for LCC double side topology has been adopted from [9]. In Fig. 5 and Fig. 6 it can be seen that the input voltage and current are in phase and similar results are obtained from the secondary side output compensating circuit. However, it is noted that the output side waveforms lag the input side because of the inductive power transfer technique. In LTSpice, the velocity analysis cannot be directly observed. Therefore, we have simulated the system using mutual and coupling information for a receiver velocity around$10m/s$.

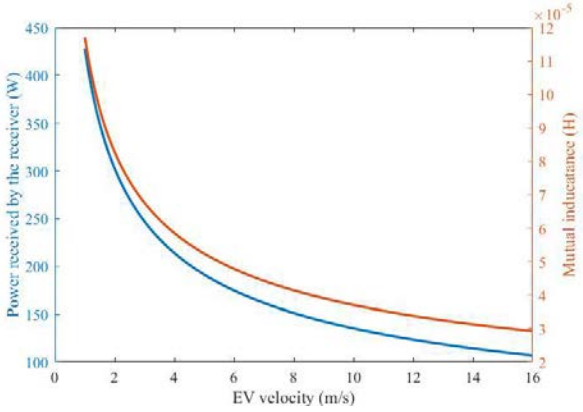

Figure 4: Variation in receiver power as a function of mutual inductance and receiver velocity

In Fig. 7, finite element analyses have been performed using ANSYS Maxwell tools. The main objective was to observe magnetic field distribution and strength across the circular coil in a fully aligned position. The analysis was performed for more than ten times scale down coil; else, the simulation requires more time to complete its iteration. The area in red colour shows that the coil can receive a very strong magnetic field from the transmitter coil. The magnetic field strength gradually decreases in the outward direction. The yellow region shows the existence of a moderate level magnetic field. While the blue region is for weak magnetic fields. The range of magnetic field flux varies from 0.02 mT to 0.7mT. For our design, if the H= 316 A-N/m and moves at the velocity of $10\ m/s$ then the receiver coil would only be able to receive 0.38 mT magnetic field flux in the specified time. A speed performance comparison has been made for a dynamically charged WPT EV system using the proposed scheme at a variable speed test in Table III. Based on simulation analysis the maximum achieved efficiency at 10

m/s is 98%. However, when the vehicle is traveling at 16 m/s, the coil to coil efficiency thus achieved is 96.9%.

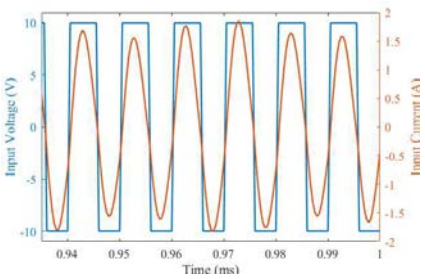

Figure 5: Input voltage and current for the primary side of the transmitter

TABLE III: PERFORMANCE FACTOR COMPARISON FOR DWPT EV SYSTEMS

Reference	[15]	[16]	[12]	[13]	[8]	[7]	[14]	Proposed work
Type of coil	Multiple coils	Multiple coils	Multiple coil transmitters	Multiple coil transmitters	Multiple coil	Multiple coil	Multiple coils	Single coil
year	2016	2016	2017	2019	2019	2019	2020	
Coil structure	Rectangular unipolar coils	Circular coils	Circular coils	DDQ coils	DD	DD	DQ coils	Circular coil
Source of uniform or less fluctuated output	Less fluctuation	Moderate fluctuation	Less fluctuation	Very Less fluctuation	Moderate fluctuation	Very Less fluctuation	Very Less Fluctuation	Less fluctuation
Compensation type	LCC type	LCC Type	SS type	LCC type	SS type	LCC type	SS	LCC Type
Speed test	No	No	No	No	No	No	Yes	Yes
Fluctuation factor	$\pm 2.9 - 7.5$ %	± 20 %	< 7.5 %	< 2 %	14.6%	1.17	1.37 % at /h 3.19 % at /h	4 km/h to 60 km/h
Efficiency	89.73%	92.5 %	80 %	90 %	-	93.41%	Not given	98%

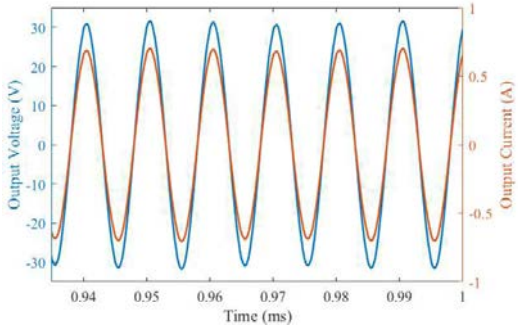

Figure 6 Output voltage and current for the primary side of the transmitter

IV. CONCLUSION

In this paper, a new way to analyze and improve receiver power has been introduced. This method adds a new constraint i.e. receiver sliding velocity while the receiver is under design consideration. By considering the velocity, the natural response of mutual inductance is not only visualized but also suggests options to improve it. Together with these constraints, the overall receiver responsivity factor can be largely improved. Then, by using LTSpice, the circuit validation is performed. It is to be noted that the capacitor C_2 is slightly different from C_1. This is done to adjust the inverter turn-off current to be minimum. FEA is performed to relate results obtained from mathematical formulations and hence it clearly states that vehicle velocity does matter while considering dynamic charging. With the adoption of this technique, future charging pad performance factors can be enhanced.

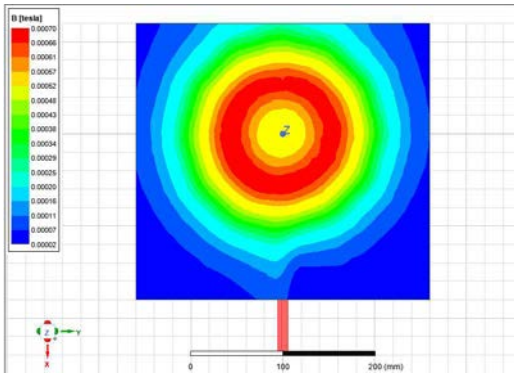

Figure 7: Finite element analysis of the circular coil using Ansys Maxwell

REFERENCES

[1] S. Niu, H. Xu, Z. Sun, Z. Y. Shao, and L. Jian, "The state-of-the-arts of wireless electric vehicle charging via magnetic resonance: principles, standards and core technologies," *Renew. Sustain. Energy Rev.*, vol. 114, p. 109302, Oct. 2019, doi: 10.1016/j.rser.2019.109302.

[2] H. Khalid *et al.*, "Analysis and Design of Series-LC-Switch Capacitor Multistage High Gain DC-DC Boost Converter for Electric Vehicle Applications," *Sustainability*, vol. 14, no. 8, p. 4495, Apr. 2022, doi: 10.3390/su14084495.

[3] W. Li, H. Zhao, J. Deng, S. Li, and C. C. Mi, "Comparison Study on SS and Double-Sided LCC Compensation Topologies for EV/PHEV Wireless Chargers," *IEEE Trans. Veh. Technol.*, vol. 65, no. 6, pp. 4429–4439, Jun. 2016, doi: 10.1109/TVT.2015.2479938.

[4] U. D. Kavimandan, V. P. Galigekere, O. Onar, M. Mohammad, B. Ozpineci, and S. M. Mahajan, "The Sensitivity Analysis of Coil Misalignment for a 200-kW Dynamic Wireless Power Transfer System with an LCC-S and LCC-P Compensation," in *2021 IEEE Transportation Electrification Conference & Expo (ITEC)*, Jun. 2021, pp. 1–8. doi: 10.1109/ITEC51675.2021.9490035.

[5] Y. Li, T. Lin, R. Mai, L. Huang, and Z. He, "Compact Double-Sided Decoupled Coils-Based WPT Systems for High-Power Applications: Analysis, Design, and Experimental Verification," *IEEE Trans. Transp. Electrif.*, vol. 4, no. 1, pp. 64–75, Mar. 2018, doi: 10.1109/TTE.2017.2745681.

[6] J. L. Villa, J. Sallan, J. F. Sanz Osorio, and A. Llombart, "High-Misalignment Tolerant Compensation Topology For ICPT Systems," *IEEE Trans. Ind. Electron.*, vol. 59, no. 2, pp. 945–951, Feb. 2012, doi: 10.1109/TIE.2011.2161055.

[7] H. Li, Y. Liu, K. Zhou, Z. He, W. Li, and R. Mai, "Uniform Power

IPT System With Three-Phase Transmitter and Bipolar Receiver for Dynamic Charging," *IEEE Trans. Power Electron.*, vol. 34, no. 3, pp. 2013–2017, Mar. 2019, doi: 10.1109/TPEL.2018.2864781.

[8] S. Cui, Z. Wang, S. Han, C. Zhu, and C. C. Chan, "Analysis and Design of Multiphase Receiver With Reduction of Output Fluctuation for EV Dynamic Wireless Charging System," *IEEE Trans. Power Electron.*, vol. 34, no. 5, pp. 4112–4124, May 2019, doi: 10.1109/TPEL.2018.2859368.

[9] W. Li, H. Zhao, S. Li, J. Deng, T. Kan, and C. C. Mi, "Integrated ${LCC} $ Compensation Topology for Wireless Charger in Electric and Plug-in Electric Vehicles," *IEEE Trans. Ind. Electron.*, vol. 62, no. 7, pp. 4215–4225, Jul. 2015, doi: 10.1109/TIE.2014.2384003.

[10] C. Bai, B. Han, B.-H. Kwon, and M. Kim, "Highly Efficient Bidirectional Series-Resonant DC/DC Converter Over Wide Range of Battery Voltages," *IEEE Trans. Power Electron.*, vol. 35, no. 4, pp. 3636–3650, Apr. 2020, doi: 10.1109/TPEL.2019.2933408.

[11] C.-T. Pan, C.-F. Chuang, and C.-C. Chu, "A Novel Transformer-less Adaptable Voltage Quadrupler DC Converter with Low Switch Voltage Stress," *IEEE Trans. Power Electron.*, vol. 29, no. 9, pp. 4787–4796, Sep. 2014, doi: 10.1109/TPEL.2013.2287020.

[12] A. Ong, P. K. S. Jayathuathnage, J. H. Cheong, and W. L. Goh, "Transmitter Pulsation Control for Dynamic Wireless Power Transfer Systems," *IEEE Trans. Transp. Electrif.*, vol. 3, no. 2, pp. 418–426, Jun. 2017, doi: 10.1109/TTE.2017.2703173.

[13] Y. Li *et al.*, "A New Coil Structure and Its Optimization Design With Constant Output Voltage and Constant Output Current for Electric Vehicle Dynamic Wireless Charging," *IEEE Trans. Ind. Informatics*, vol. 15, no. 9, pp. 5244–5256, Sep. 2019, doi: 10.1109/TII.2019.2896358.

[14] S. Song, Q. Zhang, Z. He, H. Li, and X. Zhang, "Uniform Power Dynamic Wireless Charging System With I-Type Power Supply Rail and DQ-Phase-Receiver Employing Receiver-Side Control," *IEEE Trans. Power Electron.*, vol. 35, no. 10, pp. 11205–11212, Oct. 2020, doi: 10.1109/TPEL.2020.2979029.

[15] F. Lu, H. Zhang, H. Hofmann, and C. C. Mi, "A Dynamic Charging System With Reduced Output Power Pulsation for Electric Vehicles," *IEEE Trans. Ind. Electron.*, vol. 63, no. 10, pp. 6580–6590, Oct. 2016, doi: 10.1109/TIE.2016.2563380.

[16] H. Feng, T. Cai, S. Duan, J. Zhao, X. Zhang, and C. Chen, "An LCC-Compensated Resonant Converter Optimized for Robust Reaction to Large Coupling Variation in Dynamic Wireless Power Transfer," *IEEE Trans. Ind. Electron.*, vol. 63, no. 10, pp. 6591–6601, Oct. 2016, doi: 10.1109/TIE.2016.2589922.

[17] H. Choi, M. Ciobotaru, M. Jang, and V. G. Agelidis, "Performance of Medium-Voltage DC-Bus PV System Architecture Utilizing High-Gain DC–DC Converter," *IEEE Trans. Sustain. Energy*, vol. 6, no. 2, pp. 464–473, Apr. 2015, doi: 10.1109/TSTE.2014.2382690.

[18] M. Alam, S. Mekhilef, M. Seyedmahmoudian, and B. Horan, "Dynamic Charging of Electric Vehicle with Negligible Power Transfer Fluctuation," *Energies*, vol. 10, no. 5, p. 701, May 2017, doi: 10.3390/en10050701.

[19] M. Budhia, G. A. Covic, and J. T. Boys, "Design and Optimization of Circular Magnetic Structures for Lumped Inductive Power Transfer Systems," *IEEE Trans. Power Electron.*, vol. 26, no. 11, pp. 3096–3108, Nov. 2011, doi: 10.1109/TPEL.2011.2143730.

[20] M. Budhia, G. Covic, and J. Boys, "A new IPT magnetic coupler for electric vehicle charging systems," in *IECON 2010 - 36th Annual Conference on IEEE Industrial Electronics Society*, Nov. 2010, pp. 2487–2492. doi: 10.1109/IECON.2010.5675350.

[21] M. Budhia, J. T. Boys, G. A. Covic, and C.-Y. Huang, "Development of a Single-Sided Flux Magnetic Coupler for Electric Vehicle IPT Charging Systems," *IEEE Trans. Ind. Electron.*, vol. 60, no. 1, pp. 318–328, Jan. 2013, doi: 10.1109/TIE.2011.2179274.

[22] A. Zaheer, D. Kacprzak, and G. A. Covic, "A bipolar receiver pad in a lumped IPT system for electric vehicle charging applications," in *2012 IEEE Energy Conversion Congress and Exposition (ECCE)*, Sep. 2012, pp. 283–290. doi: 10.1109/ECCE.2012.6342811.

[23] S. Kim, G. A. Covic, and J. T. Boys, "Comparison of Tripolar and Circular Pads for IPT Charging Systems," *IEEE Trans. Power Electron.*, vol. 33, no. 7, pp. 6093–6103, Jul. 2018, doi: 10.1109/TPEL.2017.2740944.